



## No-Slip Hydrodynamic Boundary Condition for Hydrophilic Particles

Christopher D.F. Honig and William A. Ducker\*

*Department of Chemical and Biomolecular Engineering, University of Melbourne, Parkville, Victoria 3010, Australia*

(Received 21 July 2006; published 11 January 2007)

We describe measurement and interpretation of the force acting on a smooth hydrophilic glass particle during rapid ( $1\text{--}100\ \mu\text{m s}^{-1}$ ) approach to, and separation from, a hydrophilic glass plate in viscous concentrated aqueous sucrose solutions ( $0.001\ \text{Pa s} < \eta < 0.090\ \text{Pa s}$ ). We find that the force is accurately described by Reynolds lubrication theory with a no-slip boundary condition, even at maximum strain rates of up to  $250\,000\ \text{s}^{-1}$ . Compared to earlier studies of hydrodynamic forces on small particles, we reduce the uncertainty in the absolute particle-plate separation by using an evanescent-wave measurement of the separation.

DOI: [10.1103/PhysRevLett.98.028305](https://doi.org/10.1103/PhysRevLett.98.028305)

PACS numbers: 47.57.J–

The Navier-Stokes equations provide the theoretical basis for the accurate description of many problems in fluid mechanics. The solution of these equations requires knowledge of the boundary conditions, and it is customary to assume a continuity of fluid velocity. Included in this assumption is continuity of fluid velocity across a solid-liquid interface, i.e., the no-slip boundary condition. However, the no-slip boundary condition has been reported to fail in sufficiently sensitive experiments, as summarized in comprehensive review articles [1–3]. The degree of deviation from the no-slip assumption is usually quantified by a fit parameter called “slip length,” which is the distance beyond the wall to which the measured velocity profile must be extrapolated to obtain zero velocity (typically  $0\text{--}100\ \text{nm}$ ) [4]. In general, disagreement between theory and experiments could be due to any one of a number of potentially inappropriate assumptions, e.g., no slip at the interface, continuity of velocity within the liquid, or homogeneous viscosity [5].

Much evidence for or against slip has been accumulated from nanometer scale ( $0\text{--}200\ \text{nm}$ ) measurements of the forces between solids that are compared to Reynolds lubrication theory (RLT). RLT predicts that the force,  $F$ , acting on a sphere radius  $R$  approaching a flat plate (or equivalent cross-cylinder geometry) is [6]

$$F = 6\pi\eta R^2 \frac{v}{h}, \quad R \gg h, \quad (1)$$

where  $h$  is the closest separation between the plate and the sphere,  $\eta$  is the viscosity of the intervening liquid, and  $v$  is the velocity of the sphere.

In wetting systems, the possibility of slip is highly controversial. Measurements of the hydrodynamic forces acting on *macroscopic* ( $R \sim 2\ \text{cm}$ ) sheets of mica [6–10] show good agreement with RLT for all separations greater than a few diameters of the solvent when using a wetting liquid. Recent publications, using micrometer-sized glass and other particles (and even some macroscopic materials), report evidence for slip for both wetting ( $\theta \sim 0$ ) [11–14], intermediate ( $\theta \sim 50$ ) [15–17], and nonwetting ( $\theta \sim 90$ )

[9,10,18,19] solid-liquid combinations. (For an exception, where slip was not found, see Ref. [20].) There are also reports that the shear rate and the surface roughness [12,20,21] influence the degree of slip. Most of these later measurements were performed using atomic force microscopes (AFMs) [22] using the colloidal probe technique [23–25].

It is important to note that an error in determining the position of the solid-liquid interface ( $h = 0$ ) directly translates into an error in determining the slip length. In traditional colloid probe measurements, the separation is not measured explicitly; the relative separation is determined from the sum of the displacement of a piezoelectric translation stage (“piezodisplacement”) and the deflection of the cantilever. The zero of separation is inferred from the shape of the deflection-piezodisplacement data [24]. Problems with this procedure include the following. (1) Resolving zero separation when there is a high-gradient force near zero separation, e.g., during hydrodynamic measurements. (2) Thermal drift in an AFM requires the user to redetermine the zero of separation in each approach or withdrawal. That is, forces at different experimental conditions (e.g., approach speeds) are usually not referenced to the same measurement of zero separation, and (3) the net separation is the small difference between two large displacements (deflection and piezodisplacement), with consequent increases in the relative errors in separation and velocity.

We have remeasured hydrodynamic forces with an AFM, but with explicit measurement of the separation between the particle and the plate. We obtain the separation from the intensity of scattering of an evanescent wave by the particle [26]. We define the zero of separation for subsequent runs under all conditions of drive velocity, viscosity, etc., from the scattering in hard wall contact.

We report measurements of the forces between glass surfaces in highly wetting aqueous sucrose solutions ( $\text{O}_2$ -plasma cleaned, contact angle  $< 5^\circ$ ), under similar conditions to Refs. [12,15]. We have only investigated smooth solids. The spherical glass particles had a radius

of about  $10\ \mu\text{m}$ , a rms roughness of  $0.7\ \text{nm}$ , and a typical maximum peak-valley roughness of  $4.5\ \text{nm}$  over  $0.01\ \mu\text{m}^2$ . The glass plate had a rms roughness of  $0.25\ \text{nm}$ , and a typical maximum peak-valley roughness of  $1.5\ \text{nm}$  over  $4\ \mu\text{m}^2$ . The sucrose viscosity was in the range  $0.001\ \text{Pa s} < \eta < 0.090\ \text{Pa s}$ .

Figure 1 shows an example of our measured data: the cantilever deflection and the scattering signal as a function of the piezodisplacement. The deflection was assumed to be proportional to the measured cantilever end slope, which was measured by the light lever technique; the scattering signal is the intensity of  $532\ \text{nm}$  light scattered into a photomultiplier tube; and the piezodisplacement is measured by a linear variable differential transducer. An important difference between the work presented here and previous work is that we used 10–100 times stiffer cantilevers ( $0.58\text{--}7.5\ \text{N m}^{-1}$ ) than used previously ( $0.05\text{--}0.6\ \text{N m}^{-1}$ ). By using a stiff cantilever, we sacrifice resolution in force but gain the following important advan-

tages: (1) we can be more confident of contacting the plate, (2) the light lever has a limited range in which the voltage or deflection is linear; we can stay in the linear regime with a stiffer spring, and (3) we attain greater particle velocities for the same drive speed because the rate of deflection of the cantilever away from the surface is reduced. This faster velocity enables a smaller relative contribution from the cantilever drag.

To obtain the separation between the particle and plate from the raw data in Fig. 1, we first convert the scattering intensity to separation by using the scattering-separation profile obtained at slow speed, where we are confident that we can measure the separation by the traditional colloidal probe method. When we do this traditional analysis, we obtain the separation using the average constant compliance of the approach and separation curves. We obtain the force (Fig. 2) by calibrating the deflection of the cantilever from the end slope signal in contact in a slow (quasistatic) approach.

The AFM measurement yields the total force acting on the cantilever. We assume that the total force is the sum of

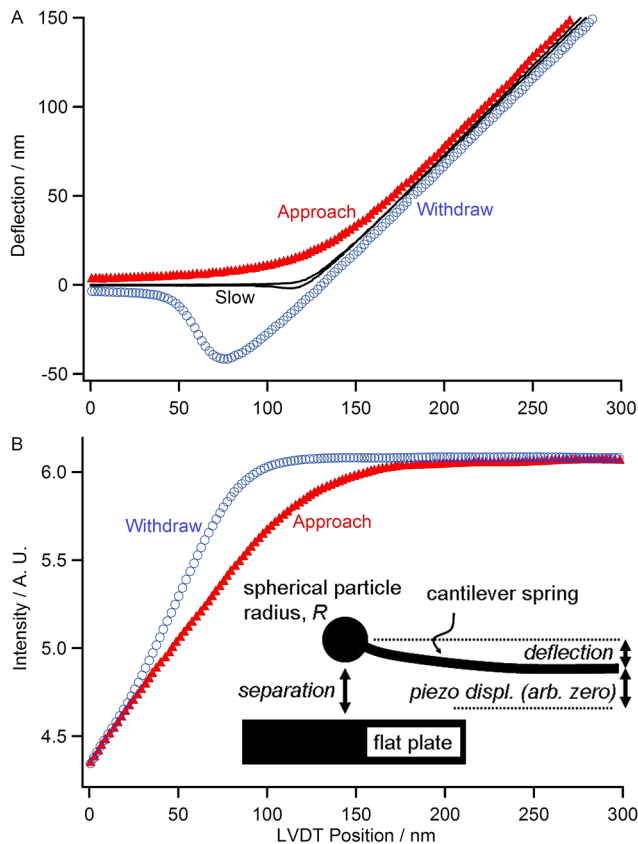


FIG. 1 (color online). Typical data set at  $10\ \mu\text{m s}^{-1}$  piezodisplacement rate. Every fifth measured point is shown. (a) Cantilever deflection as a function of piezo position. The curve labeled “slow” was measured at  $0.45\ \mu\text{m s}^{-1}$ . (b) Intensity of scattering of the evanescent wave by the particle, measured simultaneously to the data in part (a). Experimental details: Rectangular silicon cantilever (Ultrasharp Tipless NonContact NSC12)  $k = 4.5\ \text{N/m}$ , Borosilicate glass sphere  $r = 9.3\ \mu\text{m}$ , initial sucrose viscosity  $\eta = 55\ \text{mPa}$ , temperature  $20.5\ ^\circ\text{C}$ .

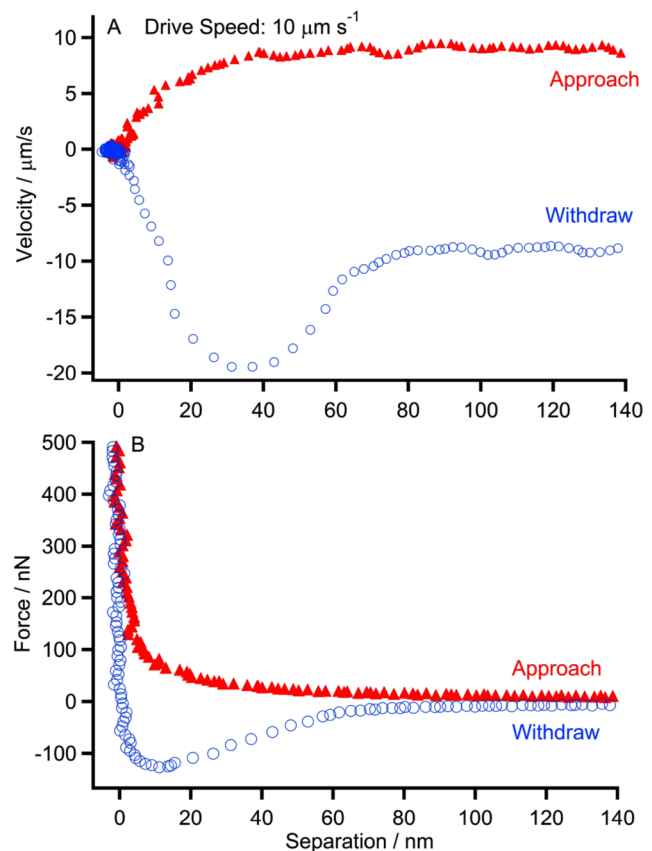


FIG. 2 (color online). Velocity and force as a function of the separation between the particle and the flat plate (same data as in Fig. 1). The separation is obtained from the light scattering, and the velocity is the time derivative of (deflection + piezodisplacement). Note that the approach and separation velocity profiles have a very different shape. Only each 5th measured point is shown.

three forces, the hydrodynamic lubrication force between the sphere and the plate, the hydrodynamic force acting on the cantilever (cantilever drag), and the surface force. (We have ignored the negligible contribution from inertia in our experiment.) We perform all experiments at  $pH$  3, where the glass has a low charge. Our experiments show that the surface forces are negligible at low approach velocity; we assume that they remain negligible at higher velocities. The cantilever drag can be measured at large separations but will change at small separations because forces change the spring deflection [27]. As in earlier work, we approximate the cantilever drag as a constant. Thus we obtain the hydrodynamic force on the sphere simply by subtracting the force at large separation [15]. The correction for the cantilever drag remains as the weakest part of the analysis: it is the principle source of systematic error at the largest separations shown in Figs. 3 and 4.

To facilitate comparison between our data and Reynolds lubrication theory, we have recast Eq. (1) so that it is linear in  $h$ :

$$\frac{v}{F_H} = \frac{1}{6\pi\eta R^2} h. \quad (2)$$

We obtain the velocity from the time derivative of (piezodisplacement + deflection); this is plotted in Fig. 2. We then plot  $v/F$  as a function of  $h$ . This has the advantage that a constant slip length appears as an offset in the entire plot, whereas a change in slope indicates a change in viscosity or more complex behavior. Figure 3 is a plot of  $v/F$  as a function of  $h$  at  $10 \mu\text{m s}^{-1}$  drive rate. Despite the fact that the  $v$  and  $F$  profile on withdrawal differ significantly from those on approach, the  $v/F$  data are the same (within error): this gives confidence that the subtraction of both the large-separation hydrodynamic force and the static force, and the measurements of separation have all

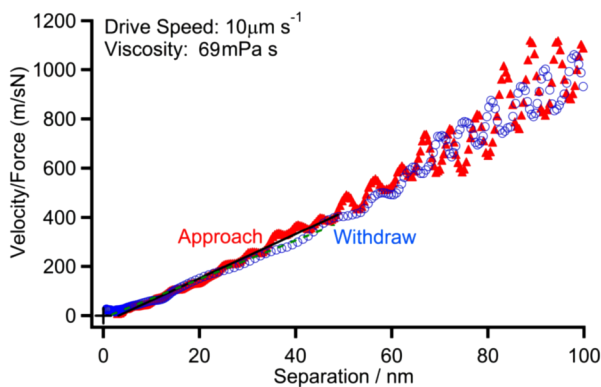


FIG. 3 (color online). Velocity/force as a function of separation between the sphere and plate. The solid triangles are data on approach, and blue hollow circles are data on withdrawal. The solid line is a linear least squares fit to the approach data in the range 5–50 nm. The  $v/F$  data are the same for approach and separation, even though the  $v$  and  $F$  contributions are quite different (Fig. 2). The 95% confidence interval of each fit passes through the origin.

been done correctly. Lines of least-squared deviation from the data in Fig. 3 have intercepts at  $v/F = 0$  of  $h = +1 \pm 1$  nm (on approach) and  $h = +1.5 \pm 1.5$  nm (on withdrawal). We do not fit data in the range 0–5 nm because the noise is larger, and because effects of the granularity of the liquid (which are not included in RLT) may become important in this range. Figure 4 is a  $v/F$  plot for a drive rate of  $100 \mu\text{m s}^{-1}$ . The intercepts of the least-squares fits are  $3 \pm 1$  nm (approach) and  $0 \pm 1$  nm (withdrawal). Combining all data, the intercept was +2 nm with a standard deviation of 2 nm.

A positive value of the intercept is consistent with a bound layer of solvent; a negative value is consistent with slip, and the error is the 95% confidence interval. So, we do not observe slip, but cannot rule out the possibility of a very thin ( $\sim 1$  nm) layer of immobile solvent. An immobile layer is consistent with the measurement of hydration forces between silica surfaces [7,24].

We performed six experiments, each with a variety of viscosities and piezodrive rates. For five of the six experiments, we observed no slip, even for maximum strain rates of up to  $250\,000 \text{ sec}^{-1}$ . In the remaining experiment, we observed a constant intercept of  $-12$  nm. After this particular experiment, scanning electron microscopy revealed that there were many nanoparticles attached to the main ( $R \sim 10 \mu\text{m}$ ) particle. A reasonable hypothesis is that in this single case one or more  $>12$  nm particles kept the  $R \sim 10 \mu\text{m}$  particle from approaching more closely than 12 nm, invalidating the reference for zero separation. In other experiments, scanning electron microscopy did not show these interfering particles. This one contaminated experiment does show how easy it is to obtain a constant slip length from particle contamination.

We have measured the hydrodynamic force as a function of solution viscosity and the drive rate. We found no significant variation in the fitted slip length as a function of viscosity in the range 0.001–0.090 Pa s. Table I shows that the slip length is not a function of drive rate in the drive range 0– $100 \mu\text{m s}^{-1}$ ; i.e., there is agreement with RLT with no slip length. This is incompatible with a slip length

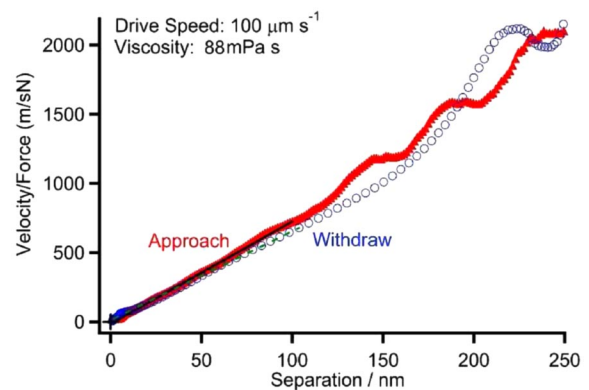


FIG. 4 (color online). Velocity/force as a function of separation at  $100 \mu\text{m s}^{-1}$  piezodisplacement rate.

TABLE I. Apparent slip length as a function of drive velocity.

Viscosity <sup>a</sup> mPa s	Drive rate $\mu\text{m s}^{-1}$	Max strain rate <sup>b</sup> $\text{s}^{-1}$	Slip length (A) <sup>c</sup> nm	Slip length (W) <sup>c</sup> nm
69	10	$1.4 \times 10^5$	$-1 \pm 1$	$1.5 \pm 1.5$
88	100	$2.5 \times 10^5$	$-5 \pm 2$	$-3 \pm 1$

<sup>a</sup>Viscosity from the slope of the  $v/F$  plot. The solution is open to the air during the experiment. In each experiment the measured viscosity is consistent with the known viscosity at the start of the experiment and then increases with time as water evaporates.

<sup>b</sup>The maximum strain rate is the strain calculated at  $h = 5$  nm.

<sup>c</sup>Average and standard deviation of 10 runs. Values  $< 0$  indicate an intercept within the fluid.  $A =$  approach runs,  $W =$  withdrawal runs.

that is a function of strain rate in the range that we have measured. Note that we maintain a constant drive rate, and not a constant velocity of the particle or a constant strain rate in each approach. The shear rate is also a function of radial position on the solid-liquid interface. The maximum shear rate at the surface ( $250\,000\text{ s}^{-1}$ ) is equivalent to the shear on the surface of a pipe, radius  $100\ \mu\text{m}$  in which water is flowing at a rate of  $6\text{ ms}^{-1}$ .

Our conclusions are in conflict with earlier work by Bonaccorso *et al.* [11,12] and Neto *et al.* [13] who found slip in very similar systems, but at a lower maximum shear rate ( $10^4\text{ s}^{-1}$ ). We think that some of the discrepancy is due to (a) a lack of a direct measure of separation in that earlier work, and (b) weak spring constants used in the earlier work, which allow for the possibility that the particle may not reach the flat plate, or if it does, it may do so when the cantilever end slope detector was in a nonlinear or uncalibrated regime.

We note that it is commonplace to discuss slip as a function of the liquid-solid contact angle. The contact angle depends on the liquid-vapor interfacial tension and the solid-vapor interfacial tension (each of which vary from liquid to liquid) as well as the solid-liquid interfacial tension (via the Young equation), whereas only measures of the solid-liquid interfacial energy are relevant to slip.

In summary, we provide strong evidence that Reynolds lubrication theory is obeyed at a smooth solid-liquid interface for a liquid that has strong interactions with the solid (sucrose-water solutions on hydroxyl-terminated glass), without the need for any fitting parameters. That is, there is no slip. In fact, the results are consistent with a very thin film of immobile liquid at the interface. Slip might be expected to occur when the interaction between the solvent and solid are weaker.

This material is based on work that was funded by both the Australian Research Council and by the National Science Foundation No. DMR 0216129.

\*Electronic address: wducker@unimelb.edu.au

- [1] C. Neto, D. Evans, and E. Bonaccorso *et al.*, Rep. Prog. Phys. **68**, 2859 (2005).  
 [2] E. Lauga, M.P. Brenner, and H.A. Stone, in *Handbook of Experimental Fluid Dynamics*, edited by J. Foss,

- C. Tropea, and A. Yarin (Springer, New York, 2005), p. 17.  
 [3] O.I. Vinogradova, Int. J. Miner. Process. **56**, 31 (1999).  
 [4] F. Brochard and P.G. de Gennes, Langmuir **8**, 3033 (1992).  
 [5] U. Raviv, P. Laurat, and J. Klein, Nature (London) **413**, 51 (2001).  
 [6] D.Y.C. Chan and R.G. Horn, J. Chem. Phys. **83**, 5311 (1985).  
 [7] R.G. Horn, D.T. Smith, and W. Haller, Chem. Phys. Lett. **162**, 404 (1989).  
 [8] J.N. Israelachvili, J. Colloid Interface Sci. **110**, 263 (1986).  
 [9] C. Cottin-Bizonne, B. Cross, and A. Steinberger *et al.*, Phys. Rev. Lett. **94**, 056102 (2005).  
 [10] C. Cottin-Bizonne, S. Jurine, and J. Baudry *et al.*, Eur. Phys. J. E **9**, 47 (2002).  
 [11] E. Bonaccorso, M. Kappl, and H.-J. Butt, Phys. Rev. Lett. **88**, 076103 (2002).  
 [12] E. Bonaccorso, H.-J. Butt, and V.S.J. Craig, Phys. Rev. Lett. **90**, 144501 (2003).  
 [13] C. Neto, V.S.J. Craig, and D.R.M. Williams, Eur. Phys. J. E **12**, S71 (2003).  
 [14] R. Pit, H. Hervet, and L. Leger, Phys. Rev. Lett. **85**, 980 (2000).  
 [15] V.S.J. Craig, C. Neto, and D.R.M. Williams, Phys. Rev. Lett. **87**, 054504 (2001).  
 [16] S. Granick, Y. Zhu, and H. Lee, Nature (London) **2**, 221 (2003).  
 [17] Y. Zhu, Langmuir **18**, 10058 (2002).  
 [18] Y. Zhu and S. Granick, Phys. Rev. Lett. **87**, 096105 (2001).  
 [19] J. Baudry, E. Charlaix, and A. Tonck *et al.*, Langmuir **17**, 5232 (2001).  
 [20] O.I. Vinogradova and G.E. Yakubov, Phys. Rev. E **73**, 045302 (2006).  
 [21] Y.X. Zhu and S. Granick, Phys. Rev. Lett. **88**, 106102 (2002).  
 [22] G. Binnig, C.F. Quate, and C. Gerber, Phys. Rev. Lett. **56**, 930 (1986).  
 [23] W.A. Ducker, T.J. Senden, and R.M. Pashley, Nature (London) **353**, 239 (1991).  
 [24] W.A. Ducker, T.J. Senden, and R.M. Pashley, Langmuir **8**, 1831 (1992).  
 [25] H.-J. Butt, Biophys. J. **60**, 1438 (1991).  
 [26] S.P. Clark, J.Y. Walz, and W.A. Ducker, Langmuir **20**, 7616 (2004).  
 [27] We were alerted to this effect by Roger Horn in February 2006.